FINAL REPORT

DEVELOPMENT OF VEHICLE MAGNETIC AIR CONDITIONER (VMAC) TECHNOLOGY

Karl A. Gschneidner, Jr., V. K. Pecharsky and David Jiles
Institute for Physical Research and Technology
Iowa State University
Ames, Iowa 50011-3020

and

Carl B. Zimm
Astronautics Corporation of America
Astronautics Technology Center
5802 Cottage Grove Rd
Madison Wi 53718-1387

DOE Contract No.: DE-FC02-98 EE 50549

DISCLAIMER

1. Feasibility Study. Phase I: Objectives and Major Accomplishments

The objective of Phase I was to explore the feasibility of the development of a new solid state refrigeration technology – magnetic refrigeration – in order to reduce power consumption of a vehicle air conditioner by 30%. The feasibility study was performed at Iowa State University (ISU) together with Astronautics Corporation of America Technology Center (ACATC), Madison, WI through a subcontract with ISU. The four technical objectives of Phase I are as follows:

i. Establish the requirements for the cost, size, weight, cooling capacity and operating conditions for the vehicle magnetic air conditioner (VMAC).
ii. Modeling and measurements of thermodynamic and magnetic properties of selected magnetic materials, to choose the most appropriate magnetic refrigerant(s) for use in the VMAC.
iii. Select a suitable permanent magnet material, perform modeling studies, build a permanent magnet configuration and measure its magnetic field strength.
iv. Determine the best heat transfer mode, mechanical configuration, and operating parameters for the VMAC.

1.1. VMAC requirements

This task was accomplished early in the project jointly by ISU and ACATC together with a major US automotive manufacturer, General Motors, [1,2]. A typical R134a automobile vapor cycle air conditioning unit ($C_2H_2F_4$ refrigerant) was used as the baseline for the VMAC performance. The major requirements are listed in Table 1. Idle is defined as a vehicle having speed 0 MPH, while down-the-road is at 50 MPH vehicle speed steady state condition.

Table 1. Operating characteristics of a typical R134a automobile air conditioner [1,2]

Vehicle vapor compression air conditioner parameters	Idealized system		Realistic system	
	Idle	Down-the-road	Idle	Down-the-road
Weight (kg)	13.6	13.6	13.6	13.6
Outside air temperature (°F)	120	100	120	100
Outside air humidity (%)	22.4	40	22.4	40
Evaporator out air temperature (°F)	70	70	70	70
System cooling capacity (kW)	3.85	6.72	3.85	6.72
System power (kW)	0.69	1.02	3.13	3.99
Overall system efficiency (% of Carnot) (Includes only the following components: 1 – compressor isentropic efficiency; 2 – condenser/gas cooler temperature effectiveness; 3 – evaporator temperature effectiveness)	**100**	**100**	**29.2**	**25.5**
System coefficient of performance (COP)	**5.58**	**6.59**	**1.23**	**1.68**
Average fuel consumption for air conditioning per passenger vehicle (gal/year)	-	-	**23.5 gal**	

The average fuel consumption was estimated [1,2] from average energy conversion efficiency of an internal combustion engine (27.5%) and average power consumption by the "realistic" air conditioner (1.8 kW, which is equivalent to ~50% of the rated average power) plus additional fuel required to carry air conditioner mass. The latter was assumed to be 10 gallons of fuel to carry each additional 100 lbs. of vehicle mass per 10,000 miles. Based on the average driving distance and average cooling period duration, approximately 20 gal/year are used to provide comfortable cooling of the passenger compartment, while ~3.5 gal/year is used to provide the energy to carry an air conditioner mass year round.

One of the big concerns with regard to automotive air conditioning is its environmental impact, which includes the two contributions. First is an indirect equivalent warming impact (IEWI) arising from fuel consumption to provide cooling and to carry VAC unit mass year round. Second is a direct refrigerant global warming potential (GWP) due to refrigerant emissions. The latter is a characteristic property of a refrigerant associated with its ability to absorb infrared rays and its lifetime in the atmosphere. A total equivalent warming impact (TEWI) is measured in kg/year and is a sum of both. In a typical R-134a vehicle air conditioner IEWI accounts for approximately 74% and GWP for 26% contribution to a TEWI. Although TEWI of an R-134a vapor cycle air conditioner is estimated to be ~4.5% of TEWI of the total average annual fuel consumption by a vehicle, its reduction is crucial especially due to a continuously expanding fleet of vehicles.

To be competitive with conventional vapor cycle automobile air conditioner VMAC must provide considerable benefits either in its operating parameters or TEWI, and preferably the both. The temperature span (120 to 70 idle or 100 to 70°F down-the-road) is feasible with a single stage VMAC even using magnetic field generated by permanent magnets. System cooling capacity (1.9 to 3.4 kW assuming 50% of the average rated power) is also likely to be achieved in the VMAC. However, VMAC configuration modeling (see section 1.4 below) shows, that this will require significant increase of the unit mass. As a matter of fact it appears that VMAC with operating parameters mentioned above would require 2 to 3-fold mass increase mainly due to rapidly rising magnet mass. On the other hand, a magnetic refrigeration device with 30% or better Carnot efficiency, much larger than unity COP, and 1 kW cooling capacity will have practically the same mass as currently available vapor compression VACs (see section 1.4). While 1 kW of cooling power may not be enough to comfortably dehumidify and cool the air inside a passenger compartment, a novel approach to provide passenger comfort by directly cooling the seats of the vehicle seems to be an ideal application for magnetic refrigeration technology. A successful magnetic vehicle passenger cooler (VMPC) unit should comfortably cool all passengers in a vehicle using a chilled heat transfer fluid and produce an order of magnitude reduction of power consumption for air conditioning. Since the GWP of magnetic refrigerant and a heat transfer fluid (water) is zero, the direct equivalent warming impact is no longer present. Combined with ~75% reduction in IWEI (~90% reduction of fuel consumption for cooling even allowing for ~10 to 15% increase of fuel consumption for slightly increased VMPC mass), TEWI could be reduced by as much as ~80% (from a total of 281.2 kg/year used by an R-134a unit to a total of 53.7 kg/year by a VMPC). Though the cost of VMPC may be initially higher than that of conventional air conditioner, our projections indicate that it will be reduced to acceptable levels once sufficient number of units are produced to fully amortize the cost of equipment to manufacture the critical components and the VMPC itself.

Therefore, the objective of Phase I to establish the cost, size, weight, cooling capacity and operating conditions of the vehicle magnetic air conditioner has been successfully accomplished.

Our research indicates that a single stage vehicle magnetic passenger cooler can be successfully designed and built within the given constraints instead of the original vehicle magnetic air conditioner. This device is conceptually different from the vehicle magnetic air conditioner envisioned at the start of the program. Full description of our approach together with the work plan leading to the construction and testing of a novel vehicle magnetic passenger cooler demonstration device (VMPCDD) is given below in section 2.

1.2. Magnetic refrigerant materials for the VMPC

This task was carried by ISU with strong collaboration and input from ACATC concerning the operating parameters of the VMPC. A highly efficient magnetic refrigerant material is at the core of a magnetic passenger cooler. Due to the use of the active magnetic regenerator (AMR) cycle (see section 1.4 below), the temperature span across the regenerator bed in the VMPC would exceed the magnetocaloric effect (MCE) of any magnetic refrigerant. However, the MCE must be large enough to allow the use of a relatively weak magnetic field of 1.5 to 2 T, which can be achieved by permanent magnet arrays. Also ideally, the MCE within the operating temperature range of the VMPC must be close to a constant value or decrease linearly with decreasing absolute temperature. Such behavior would bring the real AMR cycle closer to a thermodynamically ideal cycle further improving the VMPC efficiency. This dictates the need for careful selection of the best magnetic refrigerant materials. As large as possible adiabatic temperature change is required to produce a reasonable increase (during magnetization) and a decrease (during demagnetization) of the temperature profile across the bed to ensure an effective regeneration of the heat transfer fluid.

Based on the established operating conditions for the VMPCDD and our previous knowledge about the magnetocaloric materials for near room temperature applications, the choices were narrowed to $Gd_5(Si_{2.5}Ge_{1.5})$, a material with an ordering temperature just above 100°F (~311 K) for testing and verification of its magnetocaloric properties. This alloy belongs to a series of alloys with the overall chemical composition given as $Gd_5(Si_xGe_{1-x})_4$, where $0 \le x \le 1$ [3,4]. When $0 \le x \le 0.5$, the alloys display a giant magnetocaloric effect, which exceeds that in other known magnetic refrigerant materials by a factor of 2 to 6 [5-7]. However, the highest magnetic ordering temperature (and a maximum magnetocaloric effect) is ~285 K (54°F) for the alloy composition $Gd_5(Si_{1.985}Ge_{1.985}Ga_{0.03})$, which is too low for the VMPC application. When $x > 0.5$, the giant magnetocaloric effect no longer exists, but it still remains quite large, at least for the Gd_5Si_4 composition ($x = 1$) at ~335 K (147°F). The operating temperature of the alloys from the Gd_5Si_4-based solid solution, where Ge substitutes for Si, can be easily adjusted by changing the silicon to germanium ratio.

The measurements of the magnetic and thermodynamic properties of the $Gd_5(Si_{2.5}Ge_{1.5})$ alloy and calculation of its magnetocaloric effect confirmed that it orders magnetically at ~312 K and exhibits the magnetocaloric effect, which is large enough to be used as magnetic refrigerant material in the VMPCDD. The heat capacity in magnetic fields 0, 2, 5, 7.5 and 10 T is shown in Fig.1. It was measured in an adiabatic heat-pulse calorimeter with accuracy better than 1% [8]. The magnetocaloric effect was calculated from the total entropy functions ($S_{H=0}$ and $S_{H>0}$) as described in Ref.9. It is shown in Fig.2 for magnetic field (H) changing from 0 to 2, 5, 7.5 and 10 T. The accuracy of the magnetocaloric effect calculations was of the order of 1 to 1.5 K. This alloy undergoes a second order ferromagnetic to paramagnetic phase transition on heating, which manifests as a well-defined λ-type heat capacity anomaly in the zero magnetic field (Fig.1). As the magnetic field increases, the sharp heat capacity peak broadens and is shifted

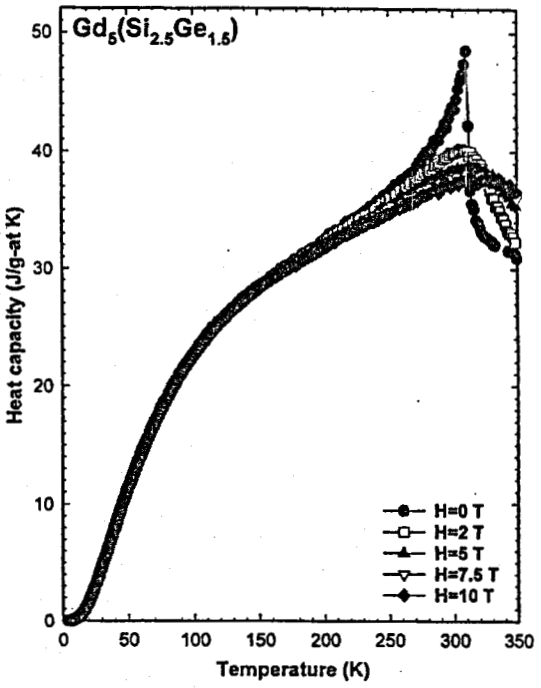

Fig.1. The heat capacity of the $Gd_5(Si_{2.5}Ge_{1.5})$ alloy measured in 0, 2, 5, 7.5 and 10 T magnetic fields.

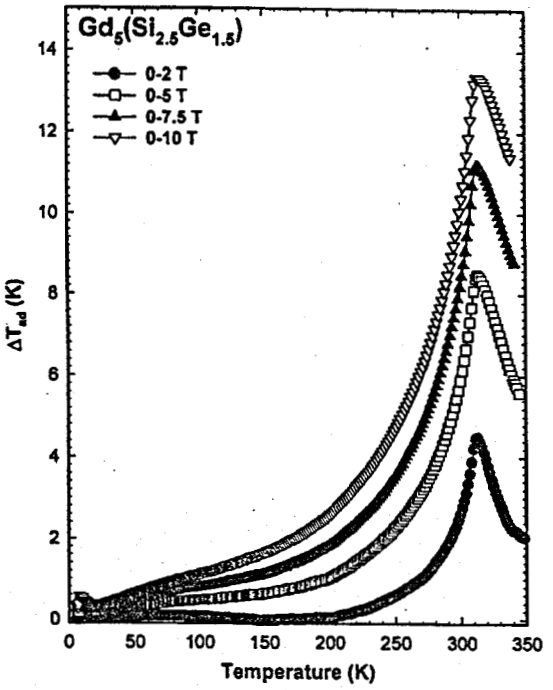

Fig.2. The magnetocaloric effect of the $Gd_5(Si_{2.5}Ge_{1.5})$ alloy for magnetic field change from 0 to 2, 5, 7.5 and 10 T.

towards higher temperature, which is typical for simple ferromagnetic materials. The magnetocaloric effect (Fig.2) also displays typical for simple ferromagnets caret-shaped peak near the ferromagnetic ordering temperature. The value of the magnetocaloric effect in $Gd_5(Si_{2.5}Ge_{1.5})$ is about 85% of that of pure Gd, and its maximum occurs at ~312 K (105°F). The magnetic hysteresis in this alloy is negligible which together with considerable magnetocaloric effect in low magnetic field makes it a good magnetic refrigerant material for the VMPC applications.

The $Gd_5(Si_{2.5}Ge_{1.5})$ alloy can be used as a single magnetic refrigerant material in magnetocaloric beds of the VMPCDD, however, its low-temperature performance can be improved by preparing a composite magnetic refrigerant containing both $Gd_5(Si_{2.5}Ge_{1.5})$ and pure Gd (the latter has much better magnetocaloric properties at the low temperature end of the VMPC). This is shown in Fig.3, where one can see the magnetocaloric effect of commercial purity Gd

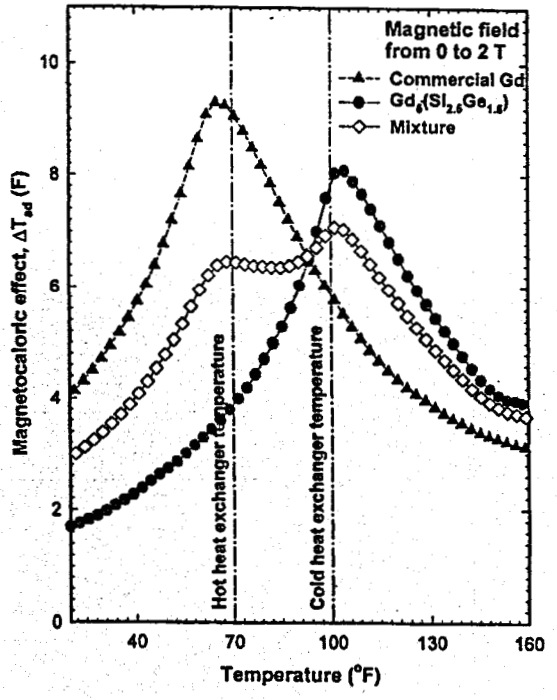

Fig.3. The magnetocaloric effect of commercial Gd, $Gd_5(Si_{2.5}Ge_{1.5})$, and a mixture of 55 wt.% Gd and 45 wt.% $Gd_5(Si_{2.5}Ge_{1.5})$ for a magnetic field change

and $Gd_5(Si_{2.5}Ge_{1.5})$ alloy for a magnetic field change from 0 to 2 T (feasible with permanent magnet configurations designed in this research, see next section). The magnetocaloric effect of a mixture of 55 wt.% Gd with 45 wt.% $Gd_5(Si_{2.5}Ge_{1.5})$ has an almost constant magnetocaloric effect, which is in excess of 6°F between 60 and 105°F. Further improvements of the magnetocaloric effect in the temperature range between 70 and 100°F are possible by introducing minor changes in both components in the mixture. The maximum magnetocaloric effect temperature of Gd can be adjusted to an exact temperature of the cold heat exchanger or even slightly lower, if necessary, by alloying it with small amounts of Er or Dy, while a further decrease of the maximum magnetocaloric effect temperature of $Gd_5(Si_{2.5}Ge_{1.5})$ can be achieved by shifting its composition to lower silicon content, $Gd_5(Si_{2.5-\delta}Ge_{1.5+\delta})$. Depending on the desired behavior of the magnetocaloric effect as a function of temperature, the overall composition of the mixture of $Gd_{1-\varepsilon}Er_\varepsilon(Dy_\varepsilon)$ and $Gd_5(Si_{2.5-\delta}Ge_{1.5+\delta})$ can be easily adjusted based on simple modeling approach described in Ref.10 and then verified experimentally. A different technique to modify the magnetocaloric properties of the Gd_5Si_4-based alloys may result in the development of a magnetic refrigerant, which is even better than $Gd_5(Si_{2.5}Ge_{1.5})$. This will be explored in Phase II.

Therefore, the objective of Phase I to select an appropriate magnetic refrigerant material(s) for VMPC operation has been successfully accomplished. Our research indicates that a single or mixed magnetic refrigerant material can be designed within the given constraints that the magnetic field strength will not exceed 2 T. Additional research on modeling and design of better magnetic refrigerants and production of the required quantities of magnetic refrigerant materials for the VMPC demonstration device will be carried in Phase II and is described below.

1.3. Permanent magnet material and configuration for the VMPC

This task was carried by ISU with a strong collaboration and input from ACATC concerning the most suitable geometry and required magnetic field strength of permanent magnet. Just as solid magnetic refrigerant replaces liquid refrigerant, a source of strong magnetic field replaces a compressor in a magnetic cooler, and therefore, it is also a critical design component of highly efficient VMPC. Earlier it was known that permanent magnet arrays (known as "magic spheres") can be fabricated to produce high intensity magnetic fields with a strength in the 2-4 T range using a spherical or hemispherical array of Nd-Fe-B permanent magnet materials with remanence of 1.2 T. These values exceed the lowest magnetic field of 1.5 T at which magnetic refrigeration has already produced significant cooling power [21].

Based on the established operating parameters of the VMPC and our knowledge of hard magnetic materials we performed critical evaluation of the properties of permanent magnet materials and computer modeling of materials and simulation of magnet arrays performance. High-performance permanent magnet materials, in particular Nd-Fe-B, which is the preferred candidate material for the VMPCDD were obtained at the beginning of Phase I. We established the demagnetization curve, which is the magnetic hysteresis loop in the second quadrant. Along with other data available from the literature, this provides sufficient information about the material's properties to carry out modeling studies of Nd-Fe-B's performance in a permanent magnet device. These data were used as input for the model calculations. We have determined the field strengths in the working volume (air gap) inside variously configured permanent magnet arrays. We have also discovered novel ways to design improved permanent magnet arrays with even higher magnetic fields than are given by the known earlier Halbach [11] and Leupold [12-19] designs. In particular we have found that the field inside of such an array can

be enhanced by the use of a soft magnetic shell around the outside of the array. This has the important role of collecting the magnetic flux to ensure that the associated magneto-static energy of the array is reduced, leading to a higher magnetic field strength inside the air gap. The major results obtained during modeling effort are briefly described below.

The finite element modeling (FEM) of selected permanent magnet arrays included "magic cylinder", "magic sphere" and other configurations expected to provide the necessary magnetic field strength over the volume required for VMAC applications. The FEM was also performed with different geometrical arrangements and magnetic material parameters, so that the magnet arrays can be optimized to obtain desired magnetic field intensity with a maximum cavity volume and minimum permanent magnet volume, mass, and therefore, cost.

The Halbach rotation theorem [11] allows us to orient the magnetization vectors of permanent magnets, so that a coherent magnetic field can be generated in the air gap inside the assembly. Fig.4 shows the direction of magnetization vectors of each permanent magnet sector according to the Halbach rotation theorem. In this example, 8 permanent magnet sectors are used to form a permanent magnet array. We calculated the magnetic flux density (Fig.5) at the center of a hollow cylindrical flux source (HCFS) for an ideal case (where $B_r = H_c$) using FEM and found that the numerical value of the flux density agrees well with the known analytical expression $B = B_r \cdot \ln(r_o/r_i)$. Here r_i and r_o are respectively the inner and outer radius of the cylindrically shaped permanent magnet array, H_c is the coercivity, and B_r is the remanence of the ferromagnetic material.

With only 8 segments in the HCFS configuration 90% of the theoretical maximum field can be obtained. This small number of sectors simplifies fabrication of practical magnetic arrays without substantial loss of magnetic field intensity. If the magnitude of the remanence is the same, then material having a higher coercivity will produce a higher magnetic field in the air gap of the array as shown in Fig. 6. Modifying the shapes of the 8 segments can enhance the magnetic flux density in the cavity of the cylinder. Insertion of soft iron in a cylindrical array

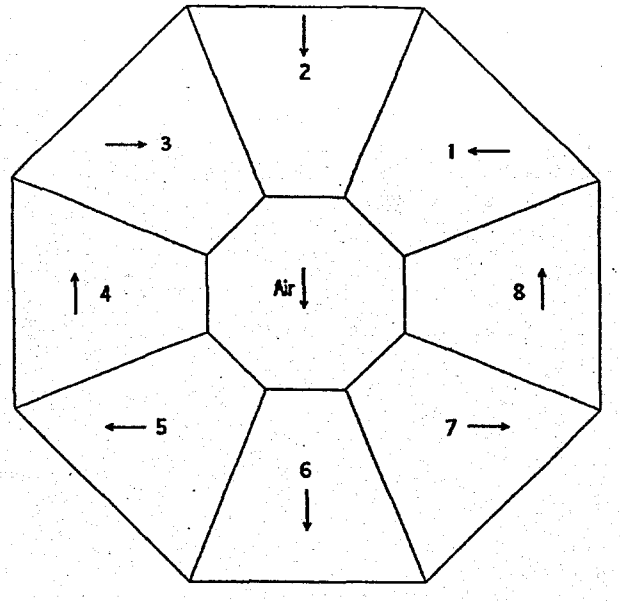

Fig.4. The Halbach arrangement of magnetization vectors for optimization of the magnetic field at the center of an array.

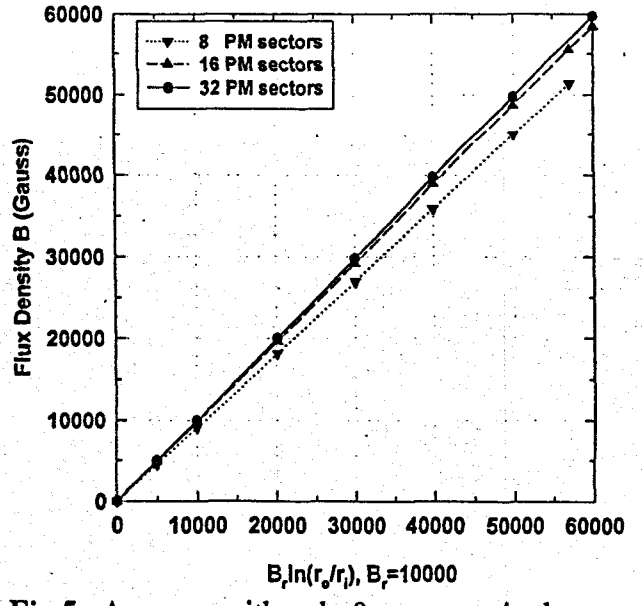

Fig.5. An array with only 8 segments in the HCFS configuration will produce ~90% of the ideal or maximum field that can be obtained.

enhances the magnitude of the magnetic field in the cavity significantly. Particularly we have found that the use of soft iron around the *outside* of the array improves the field strength *inside*.

We have shown that with certain designs, which include both inner (pole face) and outer (shell) soft iron or permalloy flux concentrators, field strengths of 2.7 to 2.9 T (Fig.7) can be obtained. This occurs in permanent magnet array when NdFeB magnet material is used in conjunction with the soft iron or permalloy flux concentrators. These field levels are substantially greater than the 2.2 Tesla obtained by Stelter [20]. More recent claims by Dexter Magnetics of a 3.2 Tesla magnet are plausible, given our results. The Stelter and Dexter Magnetics designs are, however, not particularly useful for the VMAC applications because the working volume, a cube of dimensions 5 mm x 5 mm x 5 mm (0.2 in x 0.2 in x 0.2 in) is too small. Fig.8 shows an array with slot providing access for the magnetocaloric beds and heat transfer fluid, where magnetic field strength is reduced by only ~7.5 % compared with that without a slot (Fig.7).

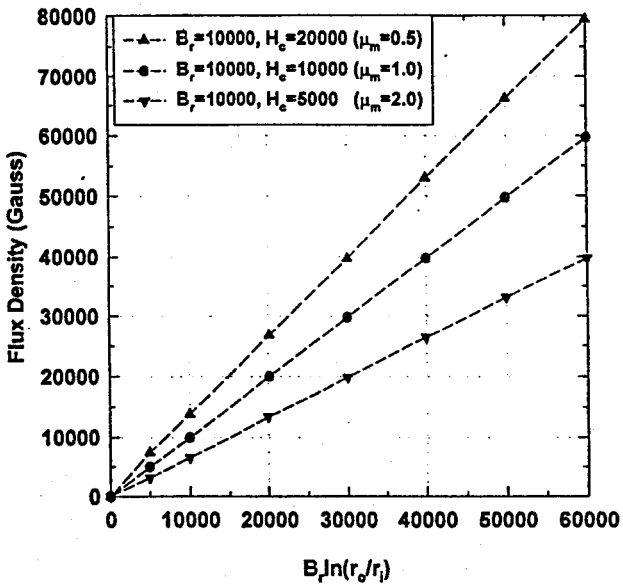

Fig.6. Calculation showing that a permanent magnet material having a higher coercivity but the same remanence will produce a higher magnetic field in an HCFS array.

Therefore, the objective of Phase I to study the feasibility of constructing a permanent magnet configuration suitable to provide 1.5 – 2.5 T magnetic field for the VMAC has been successfully accomplished. Our research indicates that a permanent magnet array can be build within the given constraints on its size, weight and cost. Additional research on modeling,

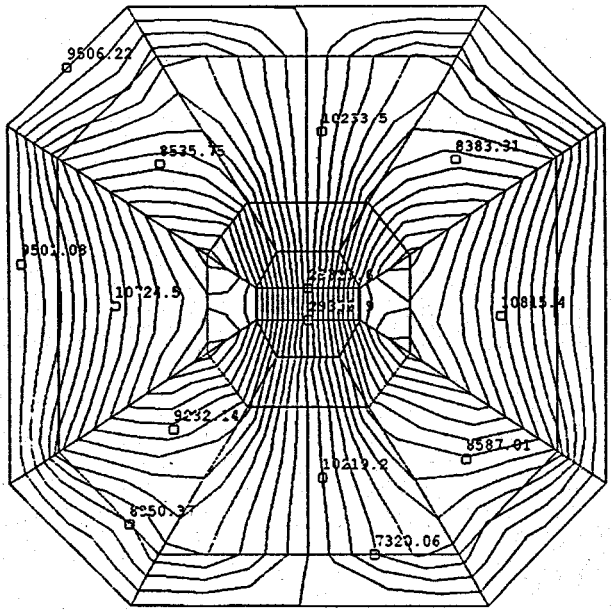

Fig.7. FEM model calculation showing a 2.9 Tesla field in a magnet array with soft magnetic

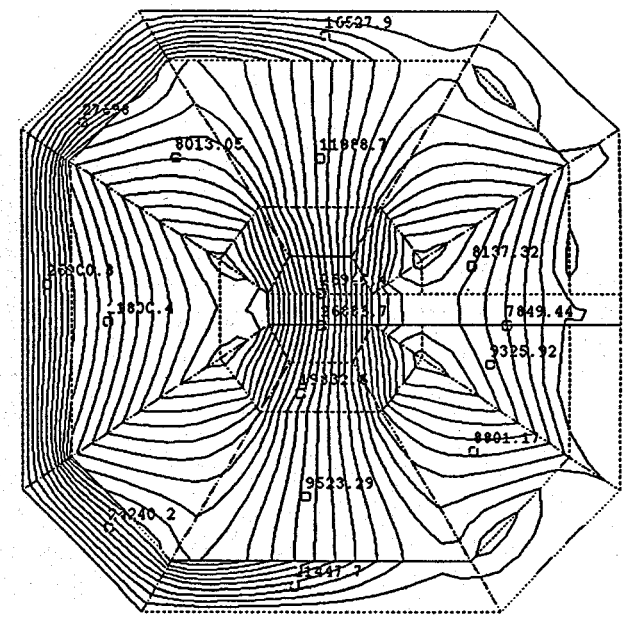

Fig.8. FEM model calculation showing a 2.7 Tesla field in a slotted magnet array with soft

design and engineering of the actual permanent magnet array for the VMAC required to minimize trade-offs and reach maximum possible magnetic field strength at minimum cost and weight penalties will be carried in Phase II as described below.

1.4. VMPC configuration and operating parameters

This task was carried by ACATC with strong collaboration and input from ISU concerning the magnetocaloric and thermodynamic properties of magnetic refrigerant materials, and the permanent magnet array parameters. The high efficiency of a magnetic refrigeration unit (MRU) arises because the compression-expansion part of the vapor cycle refrigeration is replaced by the magnetizing and demagnetizing of a magnetic material. The latter processes can be essentially dissipation free, thus approaching 100% Carnot efficiency. Our feasibility study is based on recent achievements by the ISU/ACATC team in the design, construction and operation of a proof-of-principle laboratory demonstration unit [21-23].

A magnetic vehicle passenger cooler operates by magnetizing-demagnetizing the magnetic material in continuous magnetic refrigeration cycle. Because the refrigerant is a solid it can not be pumped through a heat exchanger. The heat transfer, therefore, is usually done via a fluid passing through the magnetic refrigerant and heat exchanger. This replaces the compressor and the low boiling temperature liquid in conventional refrigeration systems. The controlling circuits and heat exchangers remain essentially the same. Unique advantages of VMPC arise from the use of the active magnetic regenerator (AMR) cycle. In the AMR cycle, a porous bed of magnetic refrigerant material acts as both the refrigerant (coolant) that produces refrigeration and the regenerator for the heat transfer fluid.

The process is operated as shown in Fig.9 for a steady state condition. For ease of understanding, assume that the hot heat exchanger is at ~22°C (75°F) and the cold heat exchanger is at ~5°C (40°F). In Fig.9a, the initial temperature profile is for the bed in its demagnetized state in zero magnetic field (dashed line). When a magnetic field is applied to the refrigerant, each particle in the bed warms because of the magnetocaloric effect to form the final magnetized bed temperature profile (solid line). The amount each particle warms is equal to the adiabatic temperature change upon magnetization at the initial temperature of the particle (ΔT_{ad}, e.g. see Figs. 2 and 3), reduced by the effect of the heat capacity of the fluid in the pores between the particles. Next, the 5°C fluid flows through the bed from the cold end to the hot end (Fig.9b). The bed is cooled by the fluid lowering the temperature profile across the bed, and the fluid in turn is warmed by the bed, emerging at a temperature close to the temperature of the bed at the warm end. This temperature is higher than 22°C, so heat is removed from the fluid at the hot heat sink as the fluid flows through the hot heat exchanger. After the fluid flow is stopped, the magnetic field is removed, cooling the bed by the magnetocaloric effect (Fig.9c). The refrigeration cycle is completed by forcing the fluid to flow from the hot to the cold end of the bed (Fig.9d). The fluid is cooled by the bed, emerging at a temperature below 5°C and removes heat from the cold sink as the fluid passes through the cold heat exchanger.

The AMR cycle outlined above has several positive features. First, the temperature span of a single stage *greatly exceeds that of the magnetocaloric effect (ΔT_{ad}) of the magnetic refrigerant.* This has been experimentally verified for near room temperature applications [21-23]. Second, because the bed acts as its own regenerator, heat need not be transferred between two separate solid assemblies, but rather between the solid particles in a single bed via the action of a fluid. The heat transfer area of a particle bed can be made very large as the particle size is reduced at

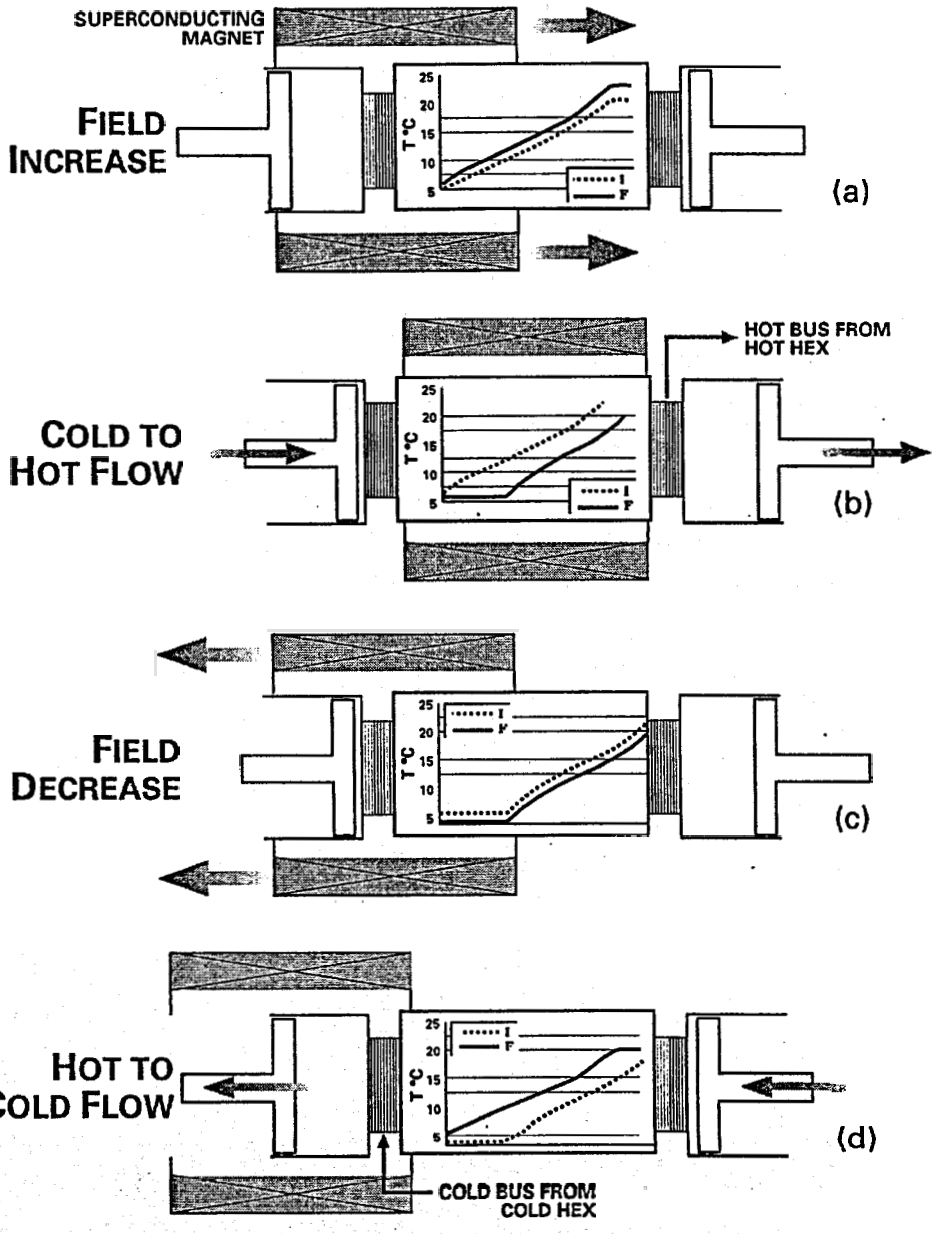

Fig.9. Four steps of the AMR cycle: magnetizing (a), flow from cold to hot (b), demagnetizing (c), and flow from hot to cold (d).

nominal fabrication cost, but with some penalty in increased resistance to flow of the heat transfer fluid. Third, *individual particles in the bed do not encounter the entire temperature span* of the stage, and hence the bed may be made into layers, each containing a magnetic material with properties optimized for a particular temperature range. This technique may enhance the cooling power or temperature span of the stage [24]. Fourth, if the refrigerant needs to be changed in response to advancing magnetic refrigerant materials technology, *only the solid particles in the AMR bed need be changed.* The capital-intensive components such as the magnet, bed drive mechanism, heat exchangers and fluid pumps need not be changed. This contrasts with the vapor cycle air conditioner, where a change in refrigerant may require extensive compressor modification or replacement.

A total of five VMPC mechanical configurations were considered. All assume use of a permanent magnet because the low temperature cooling required for superconducting magnets makes them unsuited for mobile devices. The five configurations were:

The first design consists of a is fixed magnet, with two reciprocating beds. This is the configuration that was used for the magnetic refrigerator demonstrated in 1997 [21-23] by the ISU/ACATC team (Fig.10). The geometry for this configuration is a long linear device. It requires moving the beds through seals that direct the fluid flow in the proper direction and timing to execute the AMR cycle. The seal friction in this configuration is large (see Fig.11), and at a 1.5 T field this results in a 30 % loss in efficiency. The reciprocating drive is also hard to set up off of the rotary power takeoff of conventional vehicle engines. This configuration was thus judged unsuitable for the VMPC.

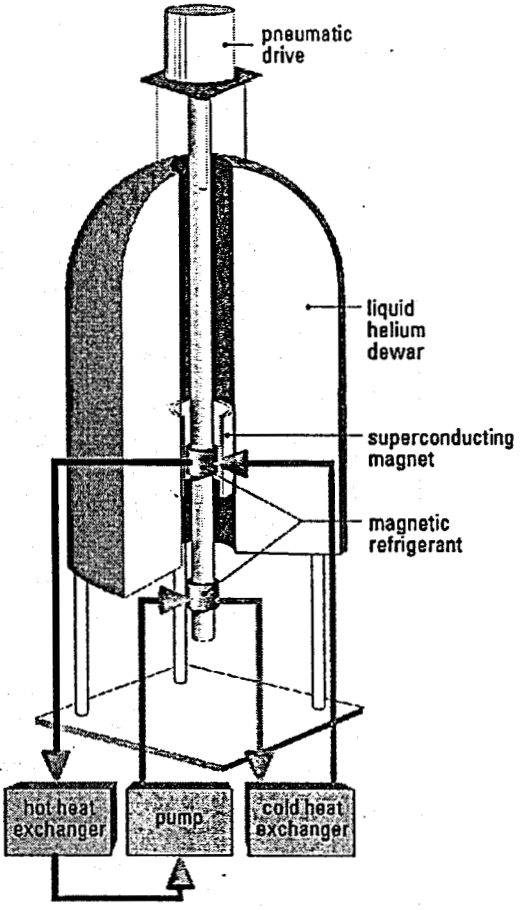

Fig.10. A schematic sketch of the reciprocating proof-of-principle magnetic refrigerator [21-23].

The second design consists of two fixed beds, with a reciprocating magnet. Sliding seals are not needed in this configuration (the flow to the beds may be controlled with valves), thereby eliminating seal friction. The problem with this configuration is that the magnet was found to weigh 5 times as much as the magnetocaloric beds. Because the inertial forces are relatively large, the vibration and drive difficulty make this configuration less attractive than rotary configurations.

The third design is for a fixed bed, surrounded by two nested ring-dipole magnets, one of which rotates. This setup was described in 1993 [25]. The field from the rotating magnet changes direction and vectorially adds to the field from the fixed magnet to produce net field magnitude proportional to $\{1 + \cos(\alpha)\}^{1/2}$, where α is the angle through which the magnet is rotated. This configuration would not have any seal friction, and could be driven easily off a rotating shaft from the engine. The problem is that the magnetic field variation would not be uniform with angle because of the vector addition. If the magnet were rotated at a constant rate, the field would be 90% or greater of its maximum value for 28.7 % of the cycle, but would be 10 % or less of its maximum value for only 6.4 % of the cycle. Thus uniform rotation of the magnet would not allow much time to carry out the low-field heat transfer part of the AMR cycle. The drive force needed to move the magnet would also be highly non-uniform.

The fourth configuration involves a fixed magnet, rotating wheel bed that threads the magnet. This configuration is commonly proposed because it would have a constant drive force and a simple drive mechanism. Published versions of this design require complex sliding seal geometries. The recent measurements of the seal friction of a reciprocating machine (the first design, Fig.11) suggests seals in this design could limit efficiency.

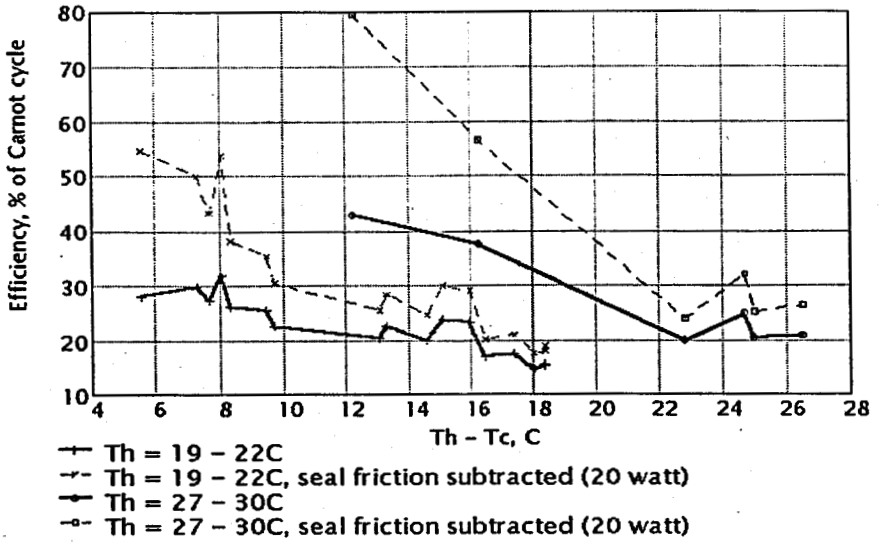

Fig.11. Effect of seal friction on the efficiency of reciprocating proof-of-principle magnetic refrigerator (magnetic field 5 T, flow rate 4 LPM).

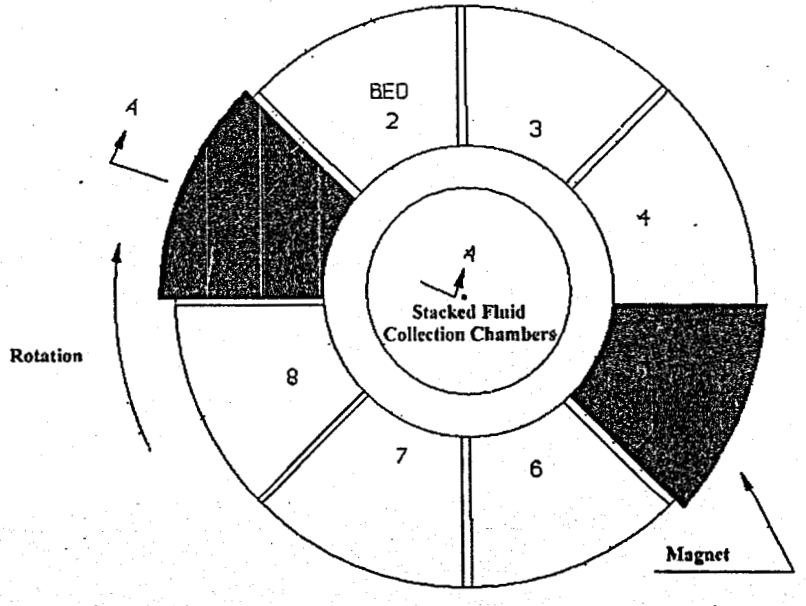

Fig.12. A schematic of VMPC demonstration device with a fixed bed and moving magnets ("whirling magnets").

The fifth design considered is a fixed wheel-shaped bed, with magnets moving over the beds(Fig.12). This configuration was found to be particularly suitable for the VMPC application. Heat transfer fluid flows in one whenever a bed is exposed to the high magnetic field from a magnet, and the flow is in the reverse direction when the bed is demagnetized. This design has the following advantages:

a) The drive motion is at constant speed and torque. Driving the system off a rotating shaft from an engine is simple.
b) The configuration is relatively compact.
c) The system can be driven at a high operating frequency without much vibration.

A theoretical model of the whirling magnet design was constructed. Correlations for heat transfer and pressure drop used in the model were verified against test results from the reciprocating magnetic refrigerator. The model of the whirling magnet configuration is more complex than the reciprocating case, however, because flow occurs as the magnets are being continuously moved, and hence the magnetic field can be changing during the flow. Much higher operating frequencies can also be obtained, so the model must also treat the entropy generation that occurs because of finite heat transfer between the magnetocaloric particles and the fluid pore volume during the rapid magnetization and demagnetization process.

Preliminary runs of the model established that 1.5 T was an appropriate magnetic field. If the field were lower, the cooling power dropped off; for higher field, the rapidly increasing magnet mass did not justify the increasing cooling power obtained.

For a 35°F (20°C) temperature span, as is typical for an air conditioner running in an down-the-road mode, gadolinium was found to be an acceptable, but not an ideal refrigerant. The limiting efficiency was found to be about 50% of Carnot for a 1.5 T magnetic field, regardless of operating frequency, fluid flow rate, particle size, bed length or fluid flow time. This efficiency was still much higher than that obtained for conventional VAC's, so the modeling proceeded using gadolinium because this material is inexpensive, readily obtainable in large quantities in powder form, and is fully characterized.

Further model runs established optimal levels for the particle size, the number of bed sectors, the magnetic field profile, and the portion of the cycle that fluid flow occurs. After these were established, scaling runs were performed to find out the effects on efficiency and cooling power of variations in the fluid flow rate, the bed length and cross sectional area. An example at constant bed mass of the effect of fluid flow rate on pressure drop (and hence efficiency) is shown in Fig.13, while the effect on cooling power is shown in Fig.14. A parametric plot could then be obtained of the tradeoff between efficiency and cooling power as the fluid flow rate and bed length were varied (Fig.15).

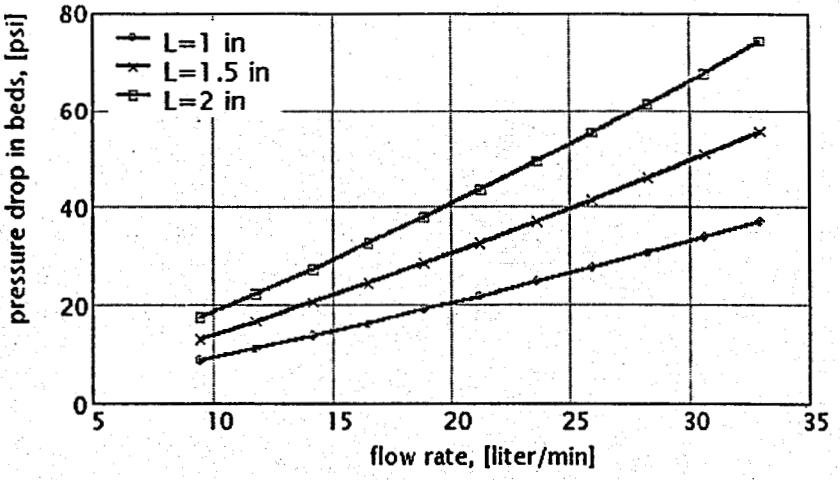

Fig.13. The effect of fluid flow rate on pressure drop in a constant mass bed for three different bed lengths: 1, 1.5 and 2 in.

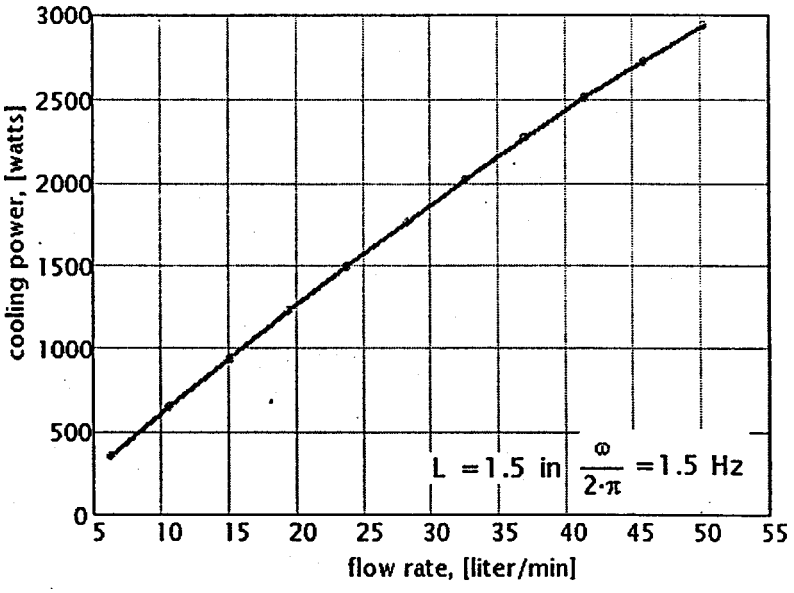

Fig.15. The effect of fluid flow rate on cooling power in a constant mass 1.5 in long bed.

A suitable design point could then be determined from the parametric plots. Even for the baseline refrigerant, gadolinium, the system performance is good (Table 2). For a ~1 kW cooling power at 30 % of Carnot efficiency using gadolinium, the bed mass is 6.9 lb., and the magnet mass is about 23.4 lb., making for a system mass of 13.7 kg which is practically the same as that of typical R-134a vapor cycle VAC (see above, section 1.1). About another 10 % should be added for the valving and fluid pump; assuming the device is driven off a pulley from the vehicle engine, no drive motor mass need be allowed for. A hot side fluid to air heat exchanger would also be needed; the fan power consumption for it has not been allowed because the fan is also used to cool the engine radiator, as was done in [1,2]. The wheel diameter would be 12

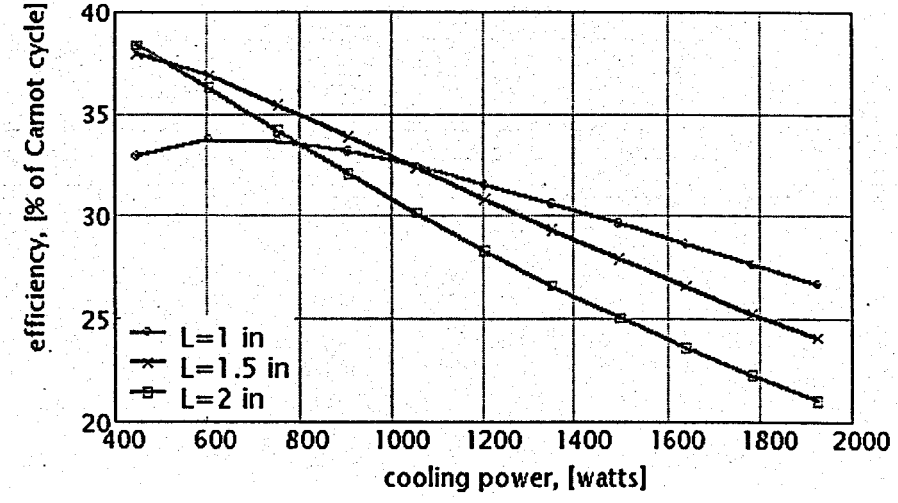

Fig.15. A parametric plot relating the efficiency and the cooling power of the VMPC for varying bed length.

inches (0.3 m), and the overall diameter of the system would be 21 inches. Improved performance from use of the enhanced magnetic refrigerants identified by ISU should result in lower system mass and size, and even lower power consumption.

Table 2. VMPC Design

Cooling Load	1100 W design, 800 W average
Cold side water inlet temperature (to seats)	15.5 C (60 F)
Aqueous fluid flow rate	19 LPM design, 14 LPM average
Hot side fluid return temperature	35 C (95 F)
Power consumption (assuming 70 % pump efficiency)	273 W design, 179 W average
System COP (W cooling / W power consumed)	4.1 design, 4.4 average
Gadolinium bed mass	3.1 kg (6.9 lb)
Magnetic field strength	1.5 T
Magnet mass	10.6 kg (23.4 lb)
System diameter	530 mm (21 in)
System height	150 mm (6 in)

In conclusion we note that the objective of Phase I to select VMPC operating parameters and mechanical configuration has been successfully accomplished. Our research shows that the current state-of-the-art in magnetic refrigerant materials, permanent magnet array design, and engineering of near room temperature AMR cycle magnetic refrigerators is sufficient for the successful design and construction of a vehicle magnetic passenger cooler demonstration device (VMPCDD).

3. References

[1] M.S. Bhatti, Soc. Automotive Engin., Paper No. 970527, 117 (1997).
[2] M.S. Bhatti, Soc. Automotive Engin., Paper No. 980289, 45 (1997).
[3] V.K. Pecharsky and K.A. Gschneidner, Jr., J. Alloys Comp., **260**, 98 (1997).
[4] V.K. Pecharsky and K.A. Gschneidner, Jr., J. Magn. Magn. Mater., **167**, L179 (1997).
[5] V.K. Pecharsky and K.A. Gschneidner, Jr., Phys. Rev. Lett., **78**, 4494 (1997).
[6] V.K. Pecharsky and K.A. Gschneidner, Jr., Appl. Phys. Lett., **70**, 3299 (1997).
[7] K.A. Gschneidner, Jr. and V.K. Pecharsky, "Active Magnetic Refrigerants Based on Gd-Si-Ge Material and Refrigeration Apparatus and Process", US Patent 5,743,095, Apr.28, 1998.
[8] V.K. Pecharsky, J.O. Moorman, and K.A. Gschneidner, Jr., Rev. Sci. Instrum., **68**, 4196 (1997).
[9] V.K.Pecharsky and K.A.Gschneidner, Jr., J. Appl. Phys., to be published.
[10] K.A.Gschneidner, Jr., V.K.Pecharsky, and S.K.Malik, Adv. Cryogen. Eng., **42A**, 475 (1996).
[11] K. Halbach, in *Proceedings of the Eighth International Workshop on Rare Earth Cobalt Permanent Magnets*, University of Dayton, Dayton, Ohio. Edited by K.J.Strnat, 1985.
[12] J.P. Clarke and H.A. Leupold, IEEE Trans. Magn. **22**, 1063 (1986).
[13] H.A. Leupold, A.S. Tilak, and E. Potenziani, IEEE Trans .Magn. **23**, 3628 (1987).

[14] H.A. Leupold and E. Potenziani, J. Appl. Phys. **63**, 3487 (1988).
[15] M.G. Abele and H.A. Leupold, J. Appl. Phys. **64**, 5998 (1988).
[16] H.A. Leupold and E. Potenziani, J. Appl. Phys. **70**, 6621 (1991).
[17] H.A. Leupold, A.S. Tilak, and E. Potenziani, IEEE Trans .Magn. **28**, 29 (1992).
[18] H.A. Leupold, A.S. Tilak, and E. Potenziani, J. Appl. Phys. **73**, 6861 (1993).
[19] H.A. Leupold, in *Rare Earth Permanent Magnets*, J.M.D.Coey (Ed.), Oxford University Press, 1996.
[20] R. Stelter, "Dipole permanent magnet structure", U.S. Patent 5,635,889, June 3, 1997.
[21] C.A. Zimm, A. Jastrab, A. Sternberg, V.K. Pecharsky, K.A. Gschneidner, Jr., M.G. Osborne, and I.E. Anderson, Adv. Cryo. Eng., **43**, 1759 (1998).
[22] K.A. Gschneidner, Jr., V.K. Pecharsky, and C.B. Zimm, Materials Technology, **12**, 145 (1997).
[23] K.A. Gschneidner, Jr., V.K. Pecharsky, and C.B. Zimm, In: Proceedings of the 50th Annual International Appliance Technical Conference at Purdue University, West Lafayette, IN, May 10-12, p.144-154 (1999).
[24] S.R. Schuricht, A.J. DeGregoria and C.B. Zimm, In: Proceedings of the 7th International Cryocooler Conference, Phillips Laboratory, Kirtland Air Force Base, NM, p. 614 (1993).
[25] J.A. Barclay, J.A. Waynert, A.J. DeGregoria, J.W. Johnson, P.J. Claybaker, "Rotary dipole active magnetic regenerative refrigerator", U.S. Patent No. 5,182,914, February 2, 1993.
[26] R.B. Farrington, R. Anderson, D.M. Blake, S.D. Burch, M.R. Cuddy, M.A. Keyser, and J.P. Rugh, "Challenges and Potential Solutions for Reducing Climate Control Loads in Conventional and Hybrid Electric Vehicles", paper presented at the 4th Intern. Vehicle Thermal Managment and Systems Conference, London (1999).
[27] ASHRAE Fundamentals, page 8.8 (1989).
[28] J.W. Mitchell and J.E. Braun, Design, Analysis and Control of Space Conditioning Equipment and Systems, Univ. of Wisconsin Instructional Notes (1999).